J|A|C|S
ARTICLES
Published on Web 12/10/2005

Electron Transfer Kinetics at Polarized Nanoscopic Liquid/Liquid Interfaces

Chenxin Cai† and Michael V. Mirkin*

Contribution from the Department of Chemistry and Biochemistry, Queens College - CUNY, Flushing, New York 11367

Received July 27, 2005; E-mail: michael_mirkin@qc.edu

Abstract: Rapid kinetics of electron transfer (ET) reactions across the interface between water and 1,2-dichloroethane were measured by steady-state voltammetry at nanopipet electrodes (50- to 400-nm orifice radius). The origins of previously reported imperfect voltammetric responses of ET reactions at micropipets were investigated. Several new experimental systems were explored, and two of them yielded high-quality voltammograms suitable for kinetic experiments. The determined standard rate constants were compared to those measured previously at polarized and nonpolarized liquid/liquid interfaces. The effect of the interfacial dimensions on the magnitude of the apparent ET rate constant is discussed. A new approach to ET kinetic measurements based on the use of the scanning electrochemical microscope with a nanopipet tip and a metallic substrate has been developed and employed to check the validity of determined kinetic parameters.

Introduction

The continuing interest in electron transfer (ET) reactions at the interface between two immiscible electrolyte solutions (ITIES) is due to their relevance to fundamental physicochemical processes (e.g., to homogeneous and heterogeneous electron transfer), electroanalysis, and important biological systems.[1] A number of electrochemical techniques including cyclic voltammetry,[2] ac impedance,[3] thin layer cell voltammetry,[4] and scanning electrochemical microscopy (SECM)[5] have been employed to study ET processes either between hydrophobic and hydrophilic molecules or between a molecule and a nanoparticle confined to immiscible aqueous and organic solutions. Several theoretical treatments of these processes have been reported.[6] However, after decades of active studies, many basic aspects of ET reactions at the liquid/liquid interface remain poorly understood. A typical example is the driving force dependence of the bimolecular rate constant.[1d] A widely accepted theoretical argument that the ET rate constant should be essentially potential-independent (because of a small voltage drop across the mixed-solvent layer separating aqueous and organic redox species[7]) was corroborated only for one experimental system,[8] while Butler−Volmer-type dependencies have been reported by several groups.[9]

A better understanding of these phenomena can be achieved by comparing kinetics of ET reactions measured at a polarized ITIES and at a nonpolarizable interface between immiscible liquids containing a common ion. In the former case, the driving force for ET reaction is determined by the externally applied voltage, while in the latter situation the overall driving force depends on the standard transfer potential and concentrations of the common ion in two phases. The kinetics of the same ET reaction may be different at polarized and nonpolarizable interfaces because of different potential profiles. A number of ET processes at nonpolarizable ITIES were studied recently by SECM.[5] Here, we use steady-state voltammetry to investigate ET reactions at the polarizable ITIES formed at the tip of a nanometer-sized pipet (Figure 1A). The pipet is filled with an aqueous solution containing a mixture of two forms of redox species (O_1 and R_1) and immersed in organic solution containing

† Permanent address: Department of Chemistry, Nanjing Normal University, Nanjing 210097, Jiangsu Province, P. R. China.

(1) For recent reviews of electron-transfer reactions at the ITIES, see: (a) Girault, H. H. In *Modern Aspects of Electrochemistry*; Bockris, J. O'M., Conway, B. E., White, R. E., Eds.; Plenum Press: New York, 1993; Vol. 25, p 1. (b) Samec, Z.; Kakiuchi, T. In *Advances in Electrochemical Science and Electrochemical Engineering*; Gerischer, H., Tobias, C. W., Eds.; VCH: New York, 1995; Vol. 4, p 297. (c) Liu, B.; Mirkin, M. V. *Anal. Chem.* **2001**, *73*, 670A. (d) Fermin, D. J.; Lahtinen, R. In *Liquid Interfaces in Chemical, Biological, and Pharmaceutical Applications*; Volkov, A. G., Ed.; Marcel Dekker: New York, 2001; p 179.
(2) (a) Samec, Z.; Marecek, V.; Weber, J. *J. Electroanal. Chem.* **1979**, *96*, 245. (b) Geblewicz, G.; Schiffrin, D. J. *J. Electroanal. Chem.* **1988**, *244*, 27.
(3) Cheng, Y.; Schiffrin, D. J. *J. Chem. Soc., Faraday Trans.* **1993**, *89*, 199.
(4) (a) Shi, C.; Anson, F. C. *J. Phys. Chem.* **1998**, *102*, 9850. (b) Barker, A. L.; Unwin, P. R. *J. Phys. Chem. B* **2000**, *104*, 2330.
(5) For reviews of SECM studies of ET at the ITIES, see: (a) Barker, A. L.; Gonsalves, M.; Unwin, P. R. *Anal. Chim. Acta* **1999**, *385*, 223. (b) Mirkin, M. V.; Tsionsky, M. In *Scanning Electrochemical Microscopy*; Bard, A. J., Mirkin, M. V., Eds.; Marcel Dekker: New York, 2001; p 299.
(6) (a) Marcus, R. A. *J. Phys. Chem.* **1990**, *94*, 1050. (b) Marcus, R. A. *J. Phys. Chem.* **1990**, *94*, 4152. (c) Marcus, R. A. *J. Phys. Chem.* **1991**, *95*, 2010. (d) Kharkats, Yu. I.; Volkov, A. G. *J. Electroanal. Chem.* **1985**, *184*, 435. (e) Kharkats, Yu. I.; Ulstrup, J. *J. Electroanal. Chem.* **1991**, *308*, 17. (f) Girault, H. H. *J. Electroanal. Chem.* **1995**, *388*, 93.
(7) (a) Girault, H. H.; Schiffrin, D. J. *J. Electroanal. Chem.* **1988**, *244*, 15. (b) Katano, H.; Maeda, K.; Senda, M. *J. Electroanal. Chem.* **1995**, *396*, 391. (c) Schmickler, W. *J. Electroanal. Chem.* **1997**, *428*, 123.
(8) Liu, B.; Mirkin, M. V. *J. Am. Chem. Soc.* **1999**, *121*, 8352.
(9) (a) Tsionsky, M.; Bard, A. J.; Mirkin, M. V. *J. Phys. Chem.* **1996**, *100*, 17881. (b) Zhang, J.; Unwin, P. R. *J. Phys. Chem. B* **2000**, *104*, 2341. (c) Barker, A. L.; Unwin, P. R.; Zhang, J. *Electrochem. Commun.* **2001**, *3*, 372. (d) Ding, Z.; Quinn, B. M.; Bard, A. J. *J. Phys. Chem. B* **2001**, *105*, 6367. (e) Zhang, Z.; Yuan, Y.; Sun, P.; Su, B.; Guo, J.; Shao, Y.; Girault, H. H. *J. Phys. Chem. B* **2002**, *106*, 6713. (f) Laforge, F. O.; Kakiuchi, T.; Shigematsu, F.; Mirkin, M. V. *J. Am. Chem. Soc.* **2004**, *126*, 15380.

10.1021/ja055091k CCC: $33.50

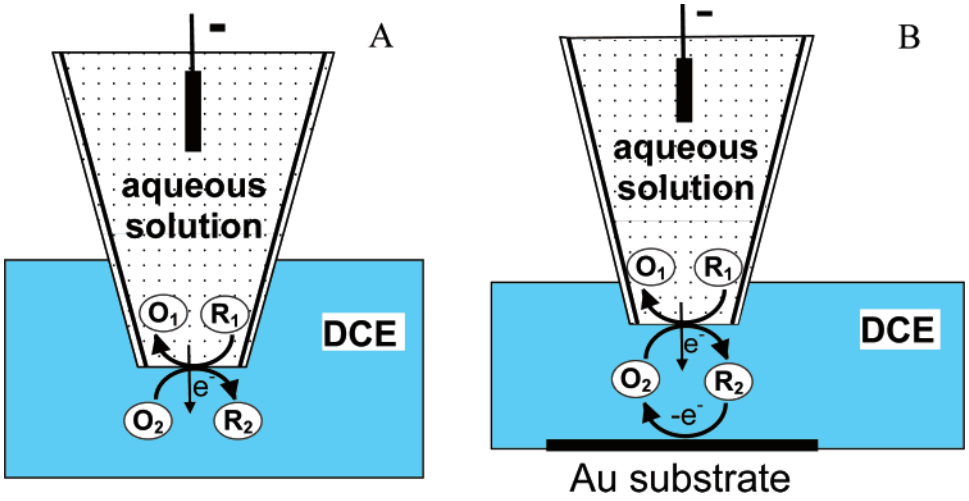

Figure 1. (A) Schematic diagram of the ET reaction across the water/1,2-dichloroethane interface formed at a nanopipet tip. (B) Feedback-mode SECM experiment with a nanopipet used as a tip electrode and a conductive Au substrate.

water-insoluble redox species (O_2). By applying a sufficiently negative potential to the internal reference electrode with respect to the external (organic) reference, one can induce interfacial ET between R_1 to O_2 species and produce an electric current across the nano-ITIES. The condition $c_{R_1} \gg c_{O_2}$ was maintained in all our experiments, so that (i) the diffusion of R_1 species inside the pipet was fast and did not control the overall current, and (2) the aqueous phase showed a metal-like behavior.[2b]

Nanopipet voltammetry offers a powerful combination of the high mass-transfer rate and very straightforward data analysis with the negligibly small effects of the resistive potential drop and double layer charging current.[10a] It was shown to be a powerful technique for investigating simple and facilitated ion transfer (IT) reactions at the ITIES;[10,11] however, no similar studies of ET have been reported to date. Moreover, previous efforts produced no well-shaped steady-state voltammograms of ET at micro-ITIES,[12] and it was concluded that "such interfaces were found not to be amenable to quantitative determinations".[12b] Here, we explore a number of combinations of various aqueous and organic redox couples and different salts employed as supporting electrolytes to identify experimental systems suitable for such studies and find out why other systems failed to yield high quality voltammograms.

Another question of interest is about compatibility of kinetic data obtained at nanometer-sized and macroscopic interfaces. The possibility of significant deviations from conventional electrochemical theory at metal electrodes smaller than ~10 nm has been discussed by Smith and White.[13a] Other authors suggested that the heterogeneous rate constants measured at larger (≥20 nm) metal nanoelectrodes may differ significantly from those determined at macroscopic electrodes because of mass transport[13b] and diffuse double layer[13c] effects specific for nanointerfaces. In studies of ITs at the ITIES, the measurements employing nanopipets yielded rate constants higher than those measured at larger interfaces. However, no strong correlation was found between the apparent IT rate and the nanopipet radius (a).[10b] Later in this article we discuss the dependence of the apparent standard ET rate constant ($k°$) on the size of a nanometer-scale interface and compare the measured rate constants with those obtained at larger polarized and non-polarized ITIES.

To separate the effects of the mass-transfer rate (which is inversely proportional to a) and the interfacial size itself on measured $k°$, we employed an SECM-based approach conceptually similar to the method used previously for ET studies at metal microelectrodes.[14] In a feedback-mode SECM experiment, the oxidized form of a redox mediator is reduced at the polarizable nanopipet-based ITIES, as shown in Figure 1B (equally, an oxidation reaction of the reduced form of the mediator can be used). The product of this reaction diffuses to the substrate electrode, where it is reoxidized. The substrate potential is constant and sufficiently positive for the oxidation reaction to be diffusion-controlled, while the tip potential is swept slowly to record a steady-state voltammogram. Such voltammograms can be obtained at different tip/substrate separation distances. Using this approach, we can vary the mass-transfer rate in two different ways: by changing the pipet radius or the tip/substrate separation distance.

Experimental Section

Chemicals. Tetrabutylammonium chloride (TBACl), potassium tetrakis(4-chlorophenyl) borate (KTPBCl), sodium tetraphenylborate (NaTPB, 99.5%), tetrabutylammonium tetraphenylborate (TBATPB, 99%), bis(triphenylphosphoranylidene)ammonium chloride (BTPPACl, 97%), tetraphenylarsonium chloride (TPAsCl, 97%), trimethylchlorosilane, 1,2-dichloroethane (DCE, 99.8%, HPLC grade), benzene (99.9+%, HPLC grade), benzonitrile (99.9%, HPLC grade), potassium hexachloroiridate (IV) (99.99%), $Na_4Fe(CN)_6$, $K_3Fe(CN)_6$ (99.99%), $FeSO_4$ (99+%), 10-methylphenothiazine (98%), and ethylenediaminetetraacetic acid (tetrasodium salt, EDTA, 98%) were all purchased from Aldrich (Milwaukee, WI). Decamethylruthenocene (DMRu; bis(pentamethylcyclopentadienyl)ruthenium, 99%) and hexaamminethenium(III) chloride were from Strem Chemicals (Newburyport, MA). Tetrahexylammonium chloride (THACl) was from Fluka; Li_2SO_4 was from J. T. Baker (Phillipsburg, NJ); and potassium hexachloroiridate(III) was from Alfa Aesar.

(10) (a) Shao, Y.; Mirkin, M. V. *J. Am. Chem. Soc.* **1997**, *119*, 8103. (b) Cai, C.; Tong, Y.; Mirkin, M. V. *J. Phys. Chem. B* **2004**, *108*, 17872.
(11) (a) Yuan, Y.; Shao, Y. *J. Phys. Chem. B* **2002**, *106*, 7809. (b) Zhan, D.; Yuan, Y.; Xiao, Y.; Wu, B.; Shao, Y. *Electrochim. Acta* **2002**, *47*, 4477.
(12) (a) Solomon, T.; Bard, A. J. *Anal. Chem.* **1995**, *67*, 2787. (b) Quinn, B.; Lahtinen, R.; Murtomäki, L.; Kontturi, K. *Electrochim. Acta* **1998**, *44*, 47.
(13) (a) Smith, C. P.; White, H. S. *Anal. Chem.* **1993**, *65*, 3343. (b) Chen, J.; Aoki, K. *Electrochem. Commun.* **2002**, *4*, 24. (c) Chen, S.; Kucernak, A. *J. Phys. Chem. B* **2002**, *106*, 9396.
(14) Mirkin, M. V.; Richards, T. C.; Bard, A. J. *J. Phys. Chem.* **1993**, *97*, 7672.

7,7,8,8-Tetracyanoquinodimethane (TCNQ, 98%) from Aldrich was recrystallized twice from acetonitrile. Nitrobenzene (99+%) from Aldrich was washed three times with deionized water. Hexaammineruthenium(II) chloride (99+%; from Aldrich) was found to be partially oxidized. It was reduced by adding Zn metal to the solution. The resulting solution of $Ru(NH_6)_3^{2+}$ was filtered in a glovebox filled with high purity nitrogen immediately before use. Tetrahexylammonium tetrakis(4-chlorophenyl)borate (THATPBCl), tetraphenylarsonium tetrakis(4-chlorophenyl)borate (TPAsTPBCl), tetrabutylammonium tetrakis-(4-chlorophenyl)borate (TBATPBCl), and bis(triphenylphosphoranylidene)ammonium tetrakis(4-chlorophenyl)borate (BTPPATPBCl) were prepared by metathesis of KTPBCl and THACl, TPAsCl, TBACl, and BTPPACl, respectively, as described previously.[15] All these salts were recrystallized thrice from acetone and used as supporting electrolytes. THATPB, TPAsTPB, and BTPPATPB were also prepared according to ref 15 and recrystallized thrice from acetone. All other chemicals were reagent-grade and were used as received. All aqueous solutions were prepared from deionized water (Milli-Q, Millipore Co.).

Pipet Preparation. The pipets of different radii were made from borosilicate capillaries (outer diameter/inner diameter ratio of 1.0/0.58) from Sutter Instrument Co. (Novato, CA) using a laser-based pipet puller (model P-2000, Sutter Instrument), as described previously.[10,16] Two halves of the same pulled capillary yielded a pair of almost identical micropipets with the same orifice radius. Several pulling programs were developed to produce short (patch-type) pipets from borosilicate glass. The shape of a micropipet and the diameter of its orifice were controlled by proper choice of the puller's five parameters. The pipets were filled with aqueous solution from the back using a small (10−25 μL) syringe. For ET experiments, 0.2-mm-diameter platinum wire (Alfa Aesar) was inserted into each pipet from the back and served as an internal reference electrode. All prepared pipets were inspected before measurements using an Olympus BH2 optical microscope to estimate the length of the narrow shaft and confirm the absence of detectable precipitate and air bubbles.

The outer glass wall of each pipet was silanized to render it hydrophobic. This was done by dipping a pipet tip into trimethylchlorosilane for 3−5 min while a flow of nitrogen sufficiently fast to produce small bubbles was passed through it from the back to avoid silanization of the inner wall of a pipet. This was crucial because the outer organic solvent gets drawn inside a glass capillary if its inner surface is hydrophobic.[16b]

Instrumentation and Procedures. Voltammetric experiments with pipets were carried out in a U-type cell inside a Faraday cage. A BAS 100B electrochemical workstation (Bioanalytical Systems, West Lafayette, IN) was employed to record cyclic voltammograms. The voltage was applied between two reference electrodes, a Pt wire inside the pipet and either a 0.25- or 0.125-μm-diameter Ag wire, which was coated with AgCl and used as an external reference. All experiments were carried out at room temperature (23 ± 2 °C). Organic solutions were purged with high purity nitrogen for at least 30 min before voltammetric measurements.

SECM experiments were carried out using a home-built instrument described previously.[8] Cell 1 with a Ag/AgTPBCl organic reference electrode was used to probe the ET between $Fe(EDTA)^{2-}$ and TCNQ:

$$\underset{\text{outer DCE solution}}{\text{Ag|AgTPBCl|10 mM THATPBCl + 0.2 mM TCNQ||}}$$

$$\underset{\text{nanopipet}}{\text{10 mM Fe(EDTA)}^{2-} + \text{1 mM Fe(EDTA)}^{-} + \text{0.025 M H}_2\text{SO}_4 +}$$

$$\text{1 M Li}_2\text{SO}_4\text{| Pt} \quad \text{(cell 1)}$$

In the negative feedback mode, Teflon was used as an insulating substrate to check the pipet geometry. In the positive feedback experiment, a 2-mm-diameter Au electrode (BAS) inserted through the bottom of the cell served as a conductive substrate. The Au substrate was biased at 200 mV (vs Ag/AgTPBCl) where the oxidation of $TCNQ^-$ was diffusion-controlled. To obtain an approach curve, the −300 mV voltage was applied between the pipet tip and the reference electrode to reduce TCNQ at a diffusion-controlled rate. The pipet tip was moved toward the substrate, and the tip current was recorded as a function of separation distance. The cyclic voltammograms were obtained by positioning the pipet tip at a suitable distance from the substrate and scanning its potential while keeping the substrate potential constant.

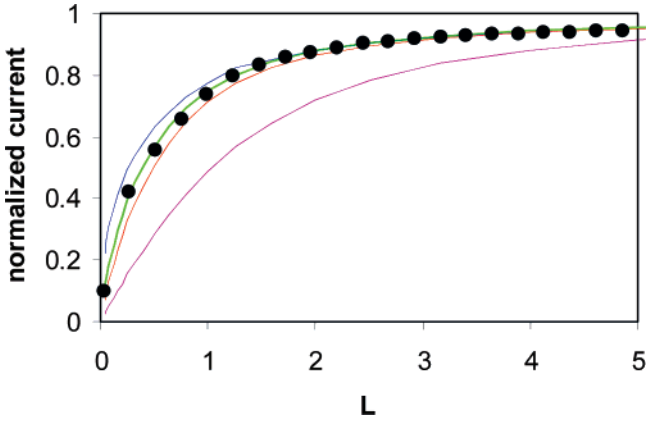

Figure 2. Experimental (●) and theoretical (solid lines) SECM current−distance curves of ET between $Fe(EDTA)^{2-}$ and TCNQ. A 255.5-nm-radius silanized nanopipet tip was biased at −300 mV and approached Teflon substrate. Theoretical curves were calculated for a = 255.5 nm and RG = 1.1 (blue), 1.5 (green), 2.0 (red), and 10 (purple). The current is normalized by the i_d value; $L = d/a$. See Cell 1 for other parameters.

Characterization of Nanopipets. The resistance of the pipet was measured to ensure that the *iR*-drop inside the narrow shaft does not affect the determined kinetic parameters. A pipet was filled with 0.1 M KCl solution and immersed in the aqueous solution of the same composition. The linear voltage sweep was applied between two Ag/AgCl reference electrodes, inside and outside the pipet. The pipet resistance was calculated from the slop of the resulting linear current versus voltage curve, as described previously.[17] In this way, the resistances were measured for a number of pipets with the radii similar to those used for ET measurements. The upper limit for the *iR*-drop in ET experiments was estimated as a product of the diffusion limiting current and the resistance value measured for a pipet of the corresponding radius. For all ET voltammograms analyzed below, the maximum *iR*-drop was <1 mV.

The employed pipets were too small to evaluate the orifice radius, a, and the ratio of the glass wall radius to the orifice radius, RG, by optical microscopy. Both parameters were extracted from the SECM approach curves. A conceptually similar procedure was described previously for micropipets[18] and nanopipets.[10b] Briefly, the approach curves were obtained using Cell 1. Unlike that in refs 10b and 18, the current across the nano-ITIES was produced by the ET reaction between TCNQ and $Fe(EDTA)^{2-}$ rather than by IT. Four theoretical approach curves (solid lines) in Figure 2 were calculated for different RG values (from 1.1 to 10).[18a] The fitting procedure showed that the radius value is really not an adjustable parameter, and a good fit could be obtained only for a specific radius value, a = 255.5 nm. The experimental data in Figure 2 fit well the theoretical curve for RG = 1.5. In contrast, the curvatures of the approach curves calculated for RG = 1.1, 2.0, and especially 10 are significantly different. Thus, the diffusion-limiting

(15) Shao, Y.; Girault, H. H. *J. Electroanal. Chem.* **1990**, *282*, 59.
(16) (a) Wei, C.; Bard, A. J.; Feldberg, S. W. *Anal. Chem.* **1997**, *69*, 4627. (b) Shao, Y.; Mirkin, M. V. *Anal. Chem.* **1998**, *70*, 3155.
(17) Shao, Y.; Liu, B.; Mirkin, M. V. *Anal. Chem.* **2000**, *72*, 510.
(18) (a) Shao, Y.; Mirkin, M. V. *J. Phys. Chem. B* **1998**, *102*, 9915. (b) Amemiya, S.; Bard, A. J. *Anal. Chem.* **2000**, *72*, 4940.

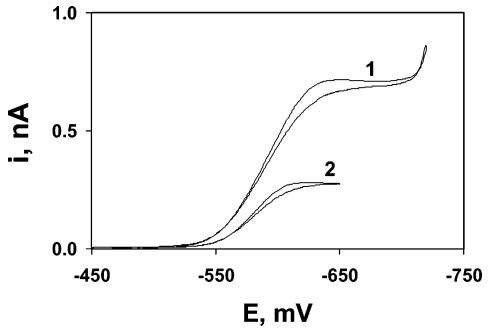

Figure 3. Voltammogram of ET between 5 mM TCNQ in nitrobenzene and aqueous $Fe(CN)_6^{4-}$ (1) and corresponding background curve obtained in the absence of TCNQ in organic phase (2). The potential sweep rate was 20 mV/s. For other parameters, see Cell 2.

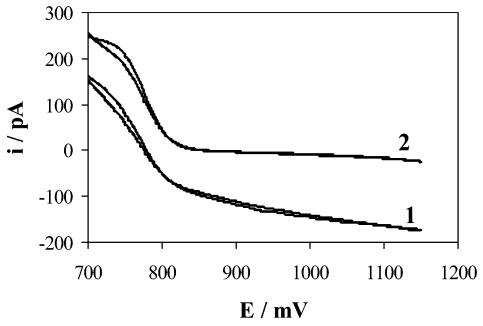

Figure 4. Voltammogram of ET between 0.5 mM DMRu in DCE and aqueous $IrCl_6^{2-}$ (1) and corresponding background curve obtained in the absence of DMRu in organic phase (2). The potential sweep rate was 20 mV/s. For other parameters, see Cell 3.

current was expressed by eq 1 with the 4.64 factor corresponding to RG = 1.5:[18a]

$$i_d = 4.64nFaDc \quad (1)$$

where F is Faraday's constant, n is the transferred charge, and D and c are the diffusion coefficient and the concentration of species in the outer solution whose transport determines the magnitude of the current. The a and RG values extracted from the SECM approach curves were consistent with those obtained from steady-state voltammograms.

Results and Discussion

Organic and Aqueous Redox Couples for ET Studies. We used Cell 2 to probe the reduction of TCNQ by $Fe(CN)_6^{4-}$ at the nano-ITIES:

Ag|AgCl|20 mM NaTPB + 10 mM NaCl||
aqueous reference solution

20 mM THATPB + x mM TCNQ||
outer organic solution

0.4 M $Fe(CN)_6^{4-}$ + 0.01 M $Fe(CN)_6^{3-}$ + 1 M Li_2SO_4|Pt
nanopipet

(cell 2)

This system has previously been employed in ET studies at macroscopic polarizable ITIES.[3] Using SECM, Zhang and Unwin obtained well-shaped approach curves from which the kinetics of this reaction at a nonpolarizable ITIES were evaluated.[9b,19] In contrast, the voltammograms obtained at micropipet-based ITIES were not well-shaped.[12] A representative curve obtained at the water/nitrobenzene interface (curve 1 in Figure 3) is not completely retraceable and exhibits a low peak instead of a flat current plateau expected for a steady-state voltammogram. The pipet radius value, $a = 0.4$ μm, was obtained from the limiting current using eq 1 with $D_{TCNQ} = 7.91 \times 10^{-6}$ cm^2/s, which was measured at a 25-μm Pt electrode. This value was somewhat larger than that observed microscopically at $\times$1000 magnification.

The origins of the imperfect shape of curve 1 can be understood by comparing it to the background voltammogram obtained for the same system and at the same pipet electrode but with no TCNQ present in organic phase (curve 2 in Figure 3). The well-defined quasi-steady-state voltammetric wave in curve 2 suggests that either the $Fe(CN)_6^{4-}$ or $Fe(CN)_6^{3-}$ ion is transferred to organic phase containing a hydrophobic cation (THA^+). Further experiments showed that the IT wave is observed only in the presence of $Fe(CN)_6^{3-}$, which apparently is the transferred species. The similar half-wave potentials of ET and IT in Figure 3 preclude quantitative studies of ET kinetics in this system.

Trying to eliminate the transfer of ferricyanide, we used different combinations of organic solvent (benzene, benzonitrile, DCE) and supporting electrolyte (TBATPB, TPAsTPB, BTPPATPB and THATPB, TBATPBCl, TPAsTPBCl, BTPPATPBCl, and THATPBCl). None of those combinations was found suitable: the transfer of $Fe(CN)_6^{3-}$ occurred in the presence of $BTPPA^+$, $TPAs^+$, or THA^+, while the use of a less hydrophobic cation (e.g., TBA^+) resulted in a polarization window too narrow for ET measurements.

A similar problem was encountered when $IrCl_6^{2-/3-}$ redox couple was used in the aqueous phase instead of $Fe(CN)_6^{3-/4-}$. The voltammogram of oxidation of decamethylruthenocene (DMRu) by $IrCl_6^{2-}$ (curve 1 in Figure 4) was obtained in Cell 3 at a silanized ~200-nm-radius pipet

Ag|AgCl|10 mM TBACl||
aqueous reference

10 mM TBATPBCl + 0.5 mM DMRu||
outer DCE solution

10 mM K_2IrCl_6 + 1 mM K_3IrCl_6 + 1.0 M Li_2SO_4|Pt
nanopipet

(cell 3)

The overlap can be seen between the ET wave observed at more positive voltages and the IT wave of the Ir complex occurring at more negative potentials. We tried to use various organic redox species with more positive standard potentials (ferrocene, 10-methylphenothiazine, ruthenocene, zinc porphyrin) to shift the ET wave in the positive direction and thus decrease the overlap. The best response was obtained with 10-methylphenothiazine dissolved in DCE, but the quality of voltammograms was not sufficiently high. Other combinations of aqueous and organic redox species, which were tested and found not suitable for quantitative kinetic measurements, include Fe^{3+}/10-methylphenothiazine, Fe^{3+}/diethylferrocene, and $Fe(EDTA)^-$/dimethylferrocene.

(19) Zhang, J.; Unwin, P. R. *Phys. Chem. Chem. Phys.* **2002**, *4*, 3820.

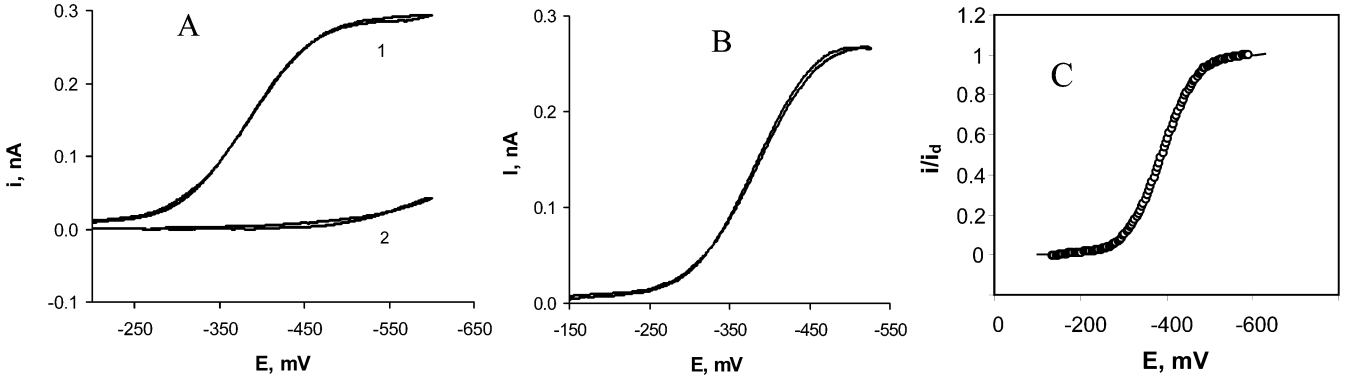

Figure 5. (A) Voltammogram of reduction of 5 mM TCNQ (in DCE) by aqueous $Ru(NH_3)_6^{2+}$ at the nanopipet-supported ITIES (1) and a background curve obtained in the absence of TCNQ (2). (B) Background-subtracted voltammogram. (C) The same curve (○) fitted to the theoretical voltammogram (solid line) calculated from eq 2. $a = 114$ nm, $\upsilon = 50$ mV/s. For other parameters, see Cell 4.

Table 1. Kinetic Parameters of the ET between $Ru(NH_3)_6^{2+}$ and TCNQ at the Water/DCE Interface Formed at a Nanopipet Tip

a, nm	c_{TCNQ}, mM	k^0, cm/s	α	$E^{0\prime}$, mV
41.0	2	1.45	0.43	−362
88.4	2	0.98	0.45	−333
103	2	0.57	0.59	−360
120	2	0.43	0.64	−349
266	2	0.43	0.49	−339
76.5	5	1.07	0.45	−371
117	5	0.57	0.60	−339
136	5	0.65	0.63	−354
148	5	0.26	0.53	−360
157	5	0.21	0.56	−369
183	5	0.31	0.57	−352
286	5	0.11	0.51	−368
482	5	0.10	0.47	−346

ET Reaction between $Ru(NH_3)_6^{2+}$ and TCNQ. Cell 4 was used to probe the reduction of TCNQ by $Ru(NH_3)_6^{2+}$ at nano-ITIES

$$\begin{array}{l}\mathrm{Ag|AgCl|20\ mM\ NaTPB + 10\ mM\ NaCl||}\\ \quad\text{aqueous reference}\\ \quad\quad\mathrm{20\ mM\ THATPB} + x\ \mathrm{mM\ TCNQ||}\\ \quad\quad\quad\text{outer DEC solution}\\ \mathrm{0.2\ M\ Ru(NH_3)_6^{2+} + 0.01\ M\ Ru(NH_3)_6^{3+} + 1\ M\ Li_2SO_4|Pt}\\ \text{nanopipet}\end{array}$$

(cell 4)

This system yielded good quality steady-state voltammograms (Figure 5A), which became suitable for quantitative kinetic analysis after the background subtraction (Figure 5B).

In Figure 5C, a good fit can be seen between the experimental voltammogram and the theory (eq 2) based on the assumptions that the interface is uniformly accessible and $D_O = D_R$ for TCNQ

$$\frac{i}{i_d} = \frac{1}{\theta + \exp[\alpha f(E - E^{\circ\prime})]/\lambda} \qquad (2)$$

where $f = F/RT$, $E^{\circ\prime}$ is the formal potential, and α is the charge-transfer coefficient of the ET reaction, $\theta = 1 + \exp[f(E - E^{\circ\prime})]$, and $\lambda = k^\circ/m = k^\circ\pi Fa^2c/i_d$. The kinetic parameters and formal potential values extracted from steady-state voltammograms are summarized in Table 1. The results shown in Table 1 were obtained for different concentrations of TCNQ and different pipet radii. As one could expect, essentially the same $E^{\circ\prime}$ value (−350 ± 20 mV; see Cell 4) was extracted from all curves. The transfer coefficient, $\alpha = 0.53 \pm 0.07$, was also constant within the limit of experimental error and independent of TCNQ concentration and pipet size. The k° values are also essentially independent of c_{TCNQ}. The mean value, $k^\circ = 0.55$ cm/s, corresponds to the standard bimolecular rate constant of $k_{12}^\circ = k^\circ/c_{Ru(NH_3)_6^{2+}} = 2.75\ M^{-1}\ cm\ s^{-1}$. This value is ∼2 orders of magnitude higher than k_{12}° values of several ET reactions measured at the micrometer-sized nonpolarizable water/DCE interface by SECM including the ET between TCNQ and ferrocyanide,[9c] and between ferrocene and ferricyanide.[9f] The rate constants measured at macroscopic ITIES were even lower, for example, $k^\circ = 9 \times 10^{-4}$ cm/s corresponding to $k_{12}^\circ = 9 \times 10^{-3}\ M^{-1}\ cm\ s^{-1}$ was reported for the ET between lutetium biphthalocyanine and $Fe(CN)_6^{3-}$.[2b]

Another unexpected result in Table 1 is a pronounced dependence of the apparent rate constant on the pipet radius. A marked increase in k° with decreasing a is at variance with the existing ET theory. Some questions about validity of these experimental findings may arise from high sensitivity of $Ru(NH_3)_6^{2+}$ species to oxygen. Although the Ru(II) solution was prepared immediately before measurements and stored under nitrogen, the complete removal of oxygen during pipet filling and voltammetric experiments was not feasible. Thus, it was difficult to ensure that the concentrations of $Ru(NH_3)_6^{2+}$ and $Ru(NH_3)_6^{3+}$ remained unchanged during the entire experiment.

ET Reaction between $Fe(EDTA)^{2-}$ and TCNQ. $Fe(EDTA)^{2-}$ is not as easily oxidized by O_2 as $Ru(NH_3)_6^{2+}$. The reduction of TCNQ by $Fe(EDTA)^{2-}$

$$\mathrm{TCNQ + Fe(EDTA)^{2-} = TCNQ^{\bullet -} + Fe(EDTA)^-} \qquad (3)$$

was carried out in Cell 5:

$$\begin{array}{l}\mathrm{Ag|AgCl|10\ mM\ TBACl\ ||}\\ \quad\text{aqueous references}\\ \quad\quad\mathrm{10\ mM\ TBATPBCl} + x\ \mathrm{mM\ TCNQ||}\\ \quad\quad\quad\text{outer DCE solution}\\ \mathrm{10\ mM\ Fe(EDTA)^{2-} + 1\ mM\ Fe(EDTA)^- +}\\ \quad\text{nanopipet}\\ \mathrm{1.0\ M\ Li_2SO_4 + 0.025\ M\ H_2SO_4|Pt}\end{array}$$

(cell 5)

This process yielded well-shaped steady-state voltammograms (Figure 6A), which, after background subtraction (Figure 6B),

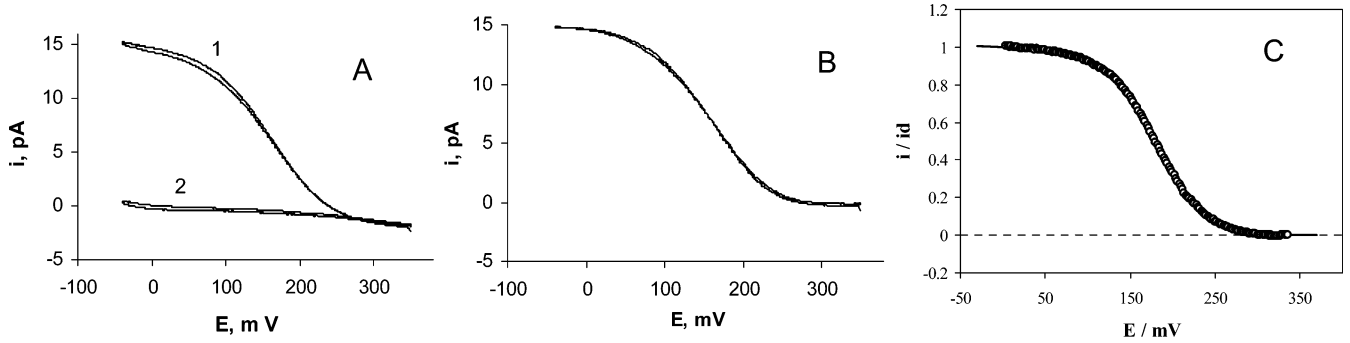

Figure 6. (A) Voltammogram of reduction of 0.2 mM TCNQ by aqueous $Fe(EDTA)^{2-}$ at the 213-nm-radius silanized pipet (1) and a background curve obtained in the absence of TCNQ (2). (B) Background-subtracted voltammogram. (C) Experimental voltammogram (○) fitted to the theory (solid line) calculated from eq 4. $\upsilon = 20$ mV/s. For other parameters, see Cell 5.

Table 2. Kinetic Parameters of the ET between 0.2 mM TCNQ and 10 mM $Fe(EDTA)^{2-}$ Obtained from Eq 2 (1u−7u) and Eq 4 (1d−7d)

voltammogram	*a*, nm	k^0, cm/s	α	E°, mV
1u	62.0	1.39	0.38	208.5
1d	62.0	1.18	0.41	210.4
2u	85.3	1.52	0.46	195.7
2d	85.3	1.30	0.53	198.4
3u	103.1	0.54	0.45	198.6
3d	103.1	0.73	0.51	202.1
4u	121.4	0.76	0.39	212.9
4d	121.4	0.66	0.43	215.2
5u	141.2	0.61	0.50	208.1
5d	141.2	0.53	0.57	212.3
6u	181.0	0.69	0.47	199.4
6d	181.0	0.56	0.53	202.4
7u	204.2	0.46	0.44	219.8
7d	204.2	0.37	0.50	223.0

were fitted to the theory (Figure 6C). As discussed earlier,[10] the kinetic parameters can be extracted from nanopipet voltammograms either by assuming the uniform accessibility of the ITIES (eq 2) or by fitting them to eq 4, which is applicable to the microdisk geometry[20]

$$\frac{i}{i_d} = \frac{1}{\theta\left[1 + \frac{\pi}{\kappa'\theta}\cdot\frac{2\kappa'\theta + 3\pi}{4\kappa'\theta + 3\pi^2}\right]} \qquad (4)$$

where $\kappa' = \pi a k^\circ/4D \exp[-\alpha n f(E - E^{\circ\prime})]$. In Table 2, the kinetic parameters were extracted by fitting the same voltammograms to either eq 2 (pipet numbers 1u, 2u, etc.) or eq 4 (pipet numbers 1d, 2d, etc.). One can see that the differences between the parameters obtained from eqs 2 and 4 are smaller than the experimental error margin. For consistency, all voltammograms discussed below (except SECM experiments) were fitted to the microdisk theory (eq 4).

A set of data in Table 3 shows that the kinetic behavior of reaction 3 is in many ways similar to that of the TCNQ/$Ru(NH_3)_6^{2+}$ system (i.e., both $E^{\circ\prime}$ and α values are essentially constant and independent of *a* and c_{TCNQ}); k° is also independent of the concentration of TCNQ but shows strong inverse correlation with *a* (Figure 7). The mean value from Table 3, $k^\circ = 0.98$ cm/s, corresponds to the standard bimolecular rate constant of $k_{12}^\circ = k^\circ/c_{Fe(EDTA)^{2-}} = 98\ M^{-1}\ cm\ s^{-1}$, that is, ∼35 times higher than the k_{12}° of the TCNQ/$Ru(NH_3)_6^{2+}$ reaction. This finding is in qualitative agreement with Marcus theory,

Table 3. Kinetic Parameters of the ET between TCNQ and 10 mM $Fe(EDTA)^{2-}$

pipet no.	c_{TCNQ}, mM	*a*, nm	k°, cm/s	α	$E^{\circ\prime}$, mV
1	0.05	139	1.01	0.54	197.4
2	0.05	145	1.32	0.34	190.2
3	0.05	178	1.85	0.39	193.6
4	0.1	58.2	1.27	0.38	205.0
5	0.1	67.8	1.19	0.38	196.7
6	0.1	69.2	1.32	0.45	190.8
7	0.1	116	1.01	0.37	184.1
8	0.1	120	1.04	0.40	191.0
9	0.1	138	0.62	0.51	203.1
10	0.1	189	0.79	0.51	207.5
11	0.1	199	0.74	0.47	192.3
12	0.1	221	0.52	0.40	184.7
13	0.1	293	0.35	0.49	179.0
14	0.1	328	0.60	0.48	200.9
15	0.1	336	0.36	0.59	211.8
16	0.2	52.2	1.91	0.38	207.3
17	0.2	54.8	1.90	0.39	204.8
18	0.2	59.7	1.76	0.37	198.7
19	0.2	62.0	1.39	0.38	208.5
20	0.2	84.1	1.42	0.42	189.6
21	0.2	103	0.84	0.45	198.6
22	0.2	106	0.91	0.34	200.1
23	0.2	131	0.72	0.42	195.3
24	0.2	157	0.90	0.45	194.8
25	0.2	169	0.62	0.49	199.4
26	0.2	181	0.69	0.47	199.4
27	0.2	204	0.46	0.44	219.8
28	0.2	234	0.45	0.47	203.9
29	0.2	242	0.36	0.55	208.6

according to which $k_{12}^\circ \approx \sqrt{k_{11}k_{22}}$,[6b] where k_{11} and k_{22} are the self-exchange rate constants for the aqueous and organic redox couples. The self-exchange rate constant for the $Fe(EDTA)^{-/2-}$ couple was reported to be higher than that for $Ru(NH_3)_6^{3+/2+}$ ($3 \times 10^4\ M^{-1}\ s^{-1}$ versus $8 \times 10^2\ M^{-1}\ s^{-1}$).[21] However, the strong inverse correlation between k° and *a* as well as the much higher k_{12}° than the previous published values are very surprising. Additional experiments were carried out to check the validity of these results.

Table 4 contains the kinetic parameter values determined for two different concentrations of $Fe(EDTA)^{2-}$ in the filling solution (i.e., 10 mM and 50 mM; $c_{Fe(EDTA)^{2-}}/c_{Fe(EDTA)^{-}} = 10$ in both cases). The average α values for two $Fe(EDTA)^{2-}$ concentrations are similar (0.44 and 0.47), and the ratio of the mean rate constant values (2.45 cm/s)/(0.52 cm/s) = 4.7 is very

(20) Oldham, K. B.; Zoski, C. G. *J. Electroanal. Chem.* **1988**, *256*, 11.

(21) Wherland, S.; Gray, H. B. In *Biological Aspects of Inorganic Chemistry*; Addison, A. W., Cullen, W., James, B. R., Dolphin, D., Eds.; Wiley: New York, 1977; p 289.

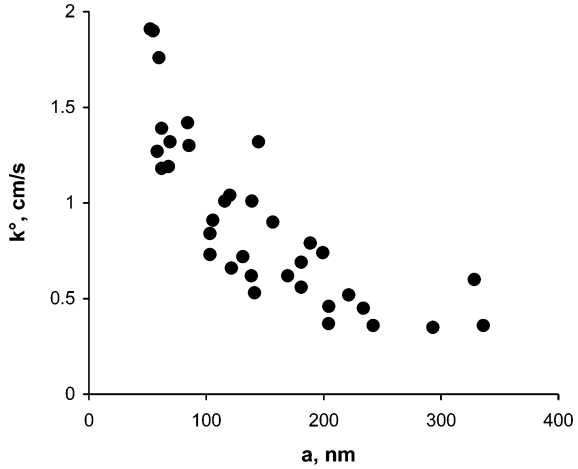

Figure 7. Dependence of the apparent standard rate constant of reaction 3 on pipet radius.

Table 4. Kinetic Parameters of Reaction 3 Measured at Different Concentrations of Aqueous Redox Species[a]

$c_{Fe(EDTA)^{2-}}$, mM	$c_{Fe(EDTA)^{-}}$, mM	*a*, nm	*k*°, cm/s	α
10	1	152	0.61	0.38
10	1	166	0.56	0.48
10	1	204	0.46	0.44
10	1	234	0.45	0.47
50	5	156	2.82	0.46
50	5	164	2.85	0.45
50	5	213	2.30	0.41
50	5	204	1.83	0.58

[a] $c_{TCNQ} = 0.2$ mM.

close to the concentration ratio, 50 mM/10 mM = 5.0. Both findings are in agreement with the theory.[2b,22]

The kinetic parameters in Table 3 were further verified by the three-point method based on the measurements of the half-wave potential, $E_{1/2}$, and two quartile potentials, $E_{1/4}$ and $E_{3/4}$.[23] This method provides two diagnostic criteria based on easily accessible values of $\Delta E_{1/4} = |E_{1/4} - E_{1/2}|$ and $\Delta E_{3/4} = |E_{1/2} - E_{3/4}|$: (i) reliable values of kinetic parameters can only be obtained if $\Delta E_{1/4} \geq 30.5$ mV and $\Delta E_{3/4} \geq 31$ mV (otherwise the corresponding voltammogram is essentially Nernstian) and (ii) the inequality $\Delta E_{3/4} \geq \Delta E_{1/4}$ holds true for any undistorted quasireversible voltammogram. All voltammograms in Table 3 satisfied both criteria. The parameter values obtained by the three-point method (not shown) were similar to those coming from curve fitting.

Our major concern was the possibility of a recessed interface similar to the "lagooned" electrode geometry.[24] If the inner pipet wall is accidentally silanized, the organic solvent may get inside the capillary. In this case, the actual area of the ITIES may be significantly larger than the geometrical area of the pipet orifice, and the rate constants obtained from steady-state voltammograms may be greatly overestimated.[24] Silanizing only the outer wall of a nanopipet without affecting its inner surface is not straightforward. To demonstrate that the interfacial area was not much larger than the geometrical area of the pipet orifice, cyclic voltammograms of reaction 3 were obtained at different scan rates (Figure 8).

All curves in Figure 8A were obtained using a 166.8-nm-radius pipet. They are sigmoidal and do not exhibit any peak even at higher scan rates (e.g., 500 mV/s). A relatively small background current corresponds to the determined pipet radius. After the background subtraction (Figure 8B), the voltammograms became essentially identical, confirming the steady-state nature of the ET reaction at the nanometer-sized ITIES as well as the absence of distortions caused by adsorption and/or resistive potential drop.

We used the SECM to further prove that the liquid/liquid interface was located at the tip of rather than inside a nanopipet. In the approach curve obtained with an insulating solid substrate (Figure 2), the current at the point of closest approach is $\sim 0.1 i_d$. This corresponds to the separation distance, $d \approx 0.025a$. Thus, the maximum possible depth of the interface "recession" inside the pipet is $\leq 0.025a$ (i.e., negligibly small). A similar conclusion can be drawn from an approach curve obtained with a conductive Au substrate (Figure 9A), where the shortest separation distance is $\sim 0.03a$.

To check if the measured kinetic parameters are independent of the mass transfer rate, steady-state voltammograms were recorded with the 206-nm pipet tip positioned at various distances from the conductive Au substrate (Figure 9B). Curve 1 obtained with a tip positioned far from the substrate ($L = d/a > 10$) was fitted to eq 4, while curves 2 and 3 were fitted to eq 5, which expresses the normalized tip current as a function of potential and separation distance:[25]

$$i_T(E,L)/i_d = \frac{0.78377}{L(\theta + 1/\kappa)} + \frac{0.68 + 0.3315\exp(-1.0672/L)}{\theta\left[1 + \frac{\pi}{\kappa\theta}\frac{2\kappa\theta + 3\pi}{4\kappa\theta + 3\pi^2}\right]} \quad (5)$$

where $\kappa = \pi k^{\circ} a \exp[-\alpha f(E - E^{\circ\prime})]/(4DI_T^c)$ and

$$I_T^c = 0.78377/L + 0.3315\exp(-1.0672/L) + 0.68 \quad (6)$$

is the diffusion-limiting current for the given L. The results summarized in Table 5 showed no apparent correlation between the measured k° and L values. Thus, the observed dependence of k° on a represents the effect of the interfacial dimensions rather than that of the mass-transfer rate.

The effect of the pipet radius on the rate constant shown in Figure 7 is significant: k° decreases by a factor of >5 over the range of a from 52 to 336 nm. The observed dependence cannot be explained by the effect of the double layer formed on the inner pipet wall. First, the diffuse layer thickness for the 1 M Li_2SO_4 filling solution (Cell 5) should be <1 nm[26] (i.e., incomparably smaller than any pipet radius in Figure 7). Second, under our experimental conditions, diffusion of redox species inside the pipet was much faster than the mass transport in the outer DCE solution, and therefore it was not rate-limiting. Additionally, the *iR*-drop inside the pipet was also negligible (<1 mV; see Experimental Section) at any a value.

Another factor to consider is the double layer formed on the outer pipet wall adjacent to the ITIES, which might affect the interfacial potential profile and consequently the ET rate.

(22) Wei, C.; Bard, A. J.; Mirkin, M. V. *J. Phys. Chem.* **1995**, *99*, 16033.
(23) Mirkin, M. V.; Bard, A. J. *Anal. Chem.* **1992**, *64*, 2293.
(24) (a) Baranski, A. S. *J. Electroanal. Chem.* **1991**, *307*, 287. (b) Oldham, K. B. *Anal. Chem.* **1992**, *64*, 646.
(25) Sun, P.; Mirkin, M. V. Manuscript in preparation.
(26) Bard, A. J.; Faulkner, L. R. *Electrochemical Methods: Fundamentals and Applications*; Wiley & Sons: New York, 2001; p 549.

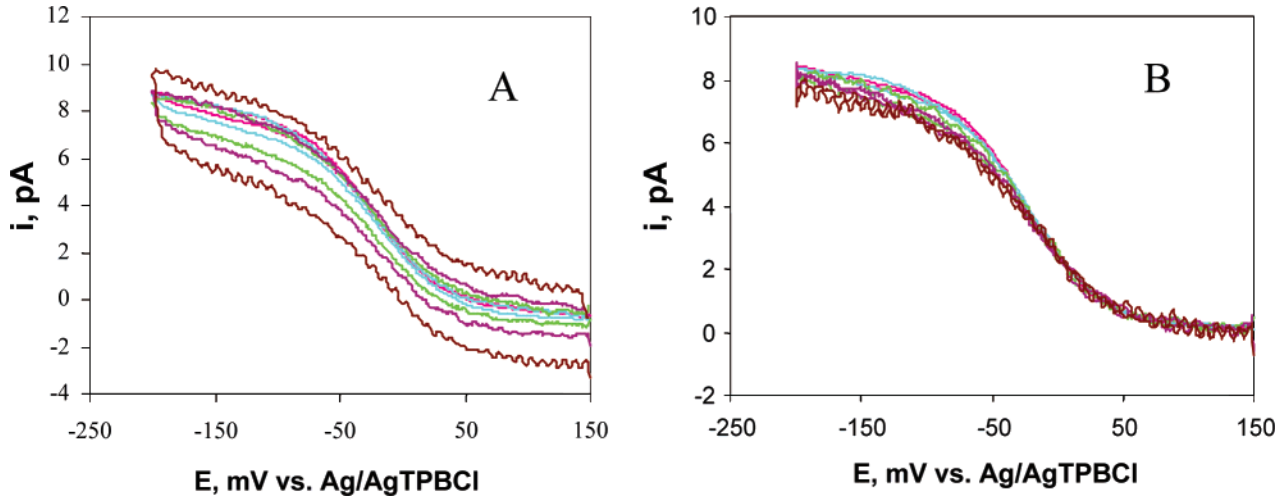

Figure 8. Cyclic voltammograms of the electron transfer between TCNQ and $Fe(EDTA)^{2-}$ at a 167-nm-radius silanized nanopipet (A) and corresponding background-subtracted curves (B). The potential sweep rate was 20 (red), 50 (blue), 100 (green), 200 (purple), and 500 (brown) mV/s. $c_{TCNQ} = 0.1$ mM, $c_{Fe(EDTA)^{2-}} = 50$ mM, $c_{Fe(EDTA)^{-}} = 5$ mM. For other parameters, see Cell 1.

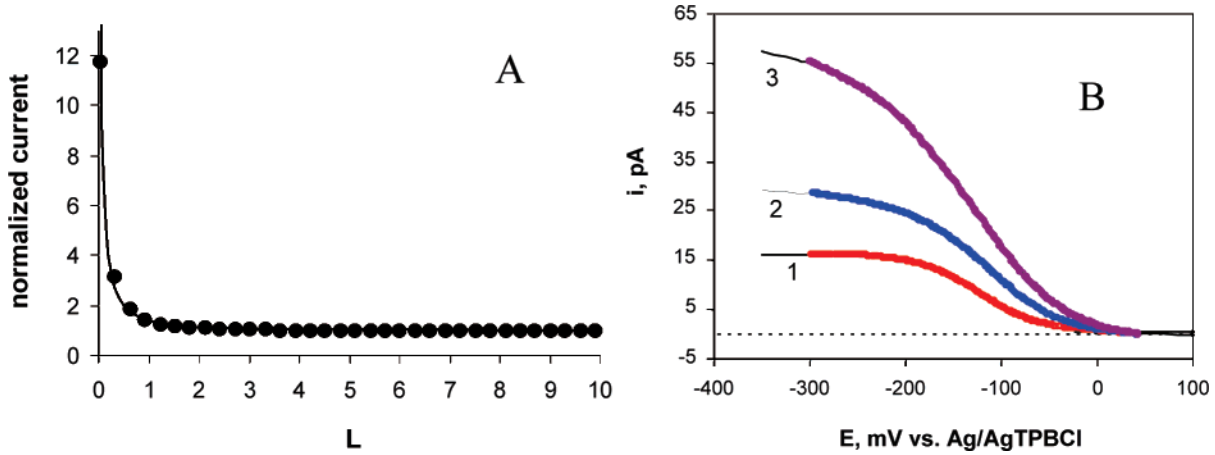

Figure 9. Experimental (●) and theoretical (sold line) current−distance curves (A) and cyclic voltammograms (B) of the ET between $Fe(EDTA)^{2-}$ and TCNQ. The tip was a 206-nm-radius silanized pipet; the substrate was a 2-mm-radius Au disk biased at +200 mV vs Ag/AgTPBCl reference. (A) The tip potential was −300 mV. Theoretical curve was calculated for RG = 1.5. (B) The normalized separation distance, *L*, was: ∞ (red), 0.5 (blue), and 0.2 (purple). The potential sweep rate was 20 mV/s. For other parameters, see Cell 1. Theoretical curve 1 was calculated from eq 4; curves 2 and 3 were calculated from eq 5.

Table 5. Kinetic Parameters of Reaction 3 Measured at Different Tip/Substrate Separation Distances

L	k°, cm/s	α
∞	0.85	0.42
0.5	0.73	0.47
0.2	1.26	0.56

However, one cannot expect any significant charge to be present on silanized glass surface exposed to DCE solution. Moreover, this factor should be equally significant for any charge-transfer reaction at a nanopipet-based ITIES (i.e., ET or IT). The lack of strong correlation between k° and *a* observed for IT reactions at similarly sized, silanized nanopipets[10b] provides additional evidence that the observed effect is not caused by the charge residing on the outer pipet wall.

The presented data can also be compared to the kinetic parameters of several rapid ET reactions recently measured at the nanometer-sized metal/solution interfaces.[25] The rate constant values obtained at solid nanoelectrodes ($a \geq 15$ nm) were somewhat higher than those previously measured at larger interfaces, but they did not vary with the electrode radius.

The inverse correlation between the apparent ET rate constant and the interfacial size may be related to the double layer structure and potential profile at the nano-ITIES. Extensive ion pairing in a low polarity solvent such as DCE results in a rather thick diffuse double layer whose effective thickness may be comparable to the radii of our smaller pipets (one should notice that the observed effect was most significant at $a \leq 100$ nm). In this case, the spherical diffuse layer model[27] may be applicable. The spherical model predicts that the double layer is compressed relative to that at a large planar surface.[27] The compressed diffuse layer in DCE may in turn result in a larger fraction of the interfacial voltage dropping between the participants of the ET reaction.

Our attempts to measure the rate of reaction 3 at the nonpolarizable water/DCE interface by SECM were unsuccessful. Negative feedback response was observed regardless of TCNQ and $Fe(EDTA)^{-}$ concentrations when perchlorate was used as a common ion in the aqueous and organic phases (see

(27) (a) Quinn, B. M.; Liljeroth, P.; Ruiz, V.; Laaksonen, T.; Kontturi, K. *J. Am. Chem. Soc.* **2003**, *125*, 6644. (b) Guo, R.; Georganopoulou, D.; Feldberg, S. W.; Donkers, R.; Murray, R. W. *Anal. Chem.* **2005**, *77*, 2662.

ref 5b for experimental details of ET measurements by SECM). To exclude the possibility that the reaction of perchlorate with some other species produced a precipitate that blocked interfacial ET, we carried out SECM experiments with tetrabutylammonium used as a common ion. However, the feedback remained negative despite a significant driving force for the ET reaction between TCNQ and $Fe(EDTA)^{2-}$. On the other hand, a number of experimental systems, which were successfully used for ET experiments at nonpolarizable ITIES under SECM conditions, do not yield good quality micropipet voltammograms. We have to conclude that many features of ET reactions at the ITIES have yet to be understood.

Conclusions

Finding a suitable experimental system for ET kinetic measurements by nanopipet voltammetry is not easy: the measured current is often disturbed by interfering ion transfer reactions and/or interfacial precipitation. In particular, the ferro/ferricyanide couple, which has been employed in many studies of ET at the ITIES, is not suitable for nanopipet voltammetry. However, by carefully choosing aqueous and organic redox couples, one can obtain well-shaped steady-state voltammograms of ET at nanopipet electrodes suitable for quantitative kinetic analysis.

Kinetic parameters of two ET reactions across the ITIES have been extracted from steady-state nanopipet voltammograms. In both cases, the obtained standard rate constants were much larger than the values previously measured at macroscopic polarized interfaces and at micrometer-sized nonpolarized ITIES. Additionally, the apparent standard rate constant increased markedly with decreasing pipet radius. In contrast, no strong correlation between k° and a was found in our previous studies of ion transfer kinetics at nanointerfaces.[10] The used nanopipets ($\sim$50- to 400-nm radius) were too large for any "nonclassical" effects that might be expected when the size of the interface becomes comparable to the molecular dimensions.[13] The possibilities of the recessed interface, incorrectly determined pipet radius, and other artifacts were also eliminated by thorough characterization of nanopipets. A new model may be necessary to explain the observed kinetic behavior.

Acknowledgment. The support of this work by the National Science Foundation (CHE-0315558 and INT-0003774) and a grant from PSC-CUNY is gratefully acknowledged. We thank Prof. David Schiffrin for helpful discussions.

JA055091K